AUG 9 1993

ORNL/NRC/LTR-93/15

ORNL
MASTER COPY

Contract Program or Project Title:	Heavy-Section Steel Technology (HSST) Program Engineering Technology Division
Subject of this Document:	Preliminary Review of the Bases for the K_{Ic} Curve in the ASME Code
Type of Document:	Letter Report
Authors:	R. K. Nanstad, J. A. Keeney, and D. E. McCabe
Date of Document:	July 12, 1993
Responsible NRC Individual and NRC Office or Division:	S. N. M. Malik (301-492-3842) Division of Engineering, U.S. Nuclear Regulatory Commission

Prepared for the
U.S. Nuclear Regulatory Commission
Washington, DC 20555
Under Interagency Agreement DOE 1886-8011-9B
NRC FIN No. B0119

OAK RIDGE NATIONAL LABORATORY
Oak Ridge, Tennessee 37831-8056
managed by
MARTIN MARIETTA ENERGY SYSTEMS, INC.
for the
U.S. DEPARTMENT OF ENERGY
under Contract No. DE-AC05-84OR21400

ORNL/NRC/LTR-93/15

PRELIMINARY REVIEW OF THE BASES FOR THE K_{Ic} CURVE IN THE ASME CODE

R. K. Nanstad
J. A. Keeney
D. E. McCabe

Manuscript Completed—July 1993
Date Published—July 1993

Prepared for the
U.S. Nuclear Regulatory Commission
Office of Nuclear Regulatory Research
under Interagency Agreement No. 18986-8011-9B

NRC Fin No. B0119

Prepared by the
OAK RIDGE NATIONAL LABORATORY
Oak Ridge, Tennessee 37831
managed by
MARTIN MARIETTA ENERGY SYSTEMS, INC.
for the
U.S. DEPARTMENT OF ENERGY
under Contract No. DE-AC05-84OR21400

PRELIMINARY REVIEW OF THE BASES FOR THE K_{Ic} CURVE IN THE ASME CODE

R. K. Nanstad
J. A. Keeney
D. E. McCabe

Oak Ridge National Laboratory
Oak Ridge, Tennessee 37831

ABSTRACT

The Heavy-Section Steel Technology Program at Oak Ridge National Laboratory includes an ongoing assessment of the margins in reactor pressure vessel (RPV) integrity analyses. Section XI of the ASME Code is referenced in 10 CFR 50; it was published in 1974, and Appendix A of that section includes both K_{Ic} and K_{Ia} curves. The K_{Ia} curve, identical to the K_{IR} curve in Section III, was constructed as a lower bound to available dynamic-initiation and crack-arrest-toughness data, while the K_{Ic} curve was constructed as a lower bound to the available static fracture toughness data for RPV steels. Use of the K_{IR} curve for establishment of the low-temperature overpressurization setpoint is beginning to constrain the operating window for some RPVs, and proposals have been made which essentially incorporate the use of the K_{Ic} curve for establishment of that setpoint. The objective of this initial study is to review the bases used for establishment of the K_{Ic} curve by comparing the data reported in EPRI NP-719-SR to the graphical plots in the EPRI report and in Appendix A of Section XI. A few errors were found in the EPRI NP-719-SR tabular data which were corrected, and a corrected data base has been generated. A plot of the corrected data base indicates that the EPRI K_{Ic} curve is not a lower bound to all the data. Preliminary statistical analyses of the corrected data using a Weibull-based procedure gives a 99% confidence curve that appears to be a good representation of a lower-bound curve to the data. Further investigations in this area are underway and involve the collection of additional fracture toughness data, both valid K_{Ic} and elastic-plastic K_{Jc} results, to provide a larger data base and to evaluate the utility of K_{Jc} data in this regard. Additionally, a similar examination of the K_{Id} and K_{Ia} data used to construct the K_{Ia} (= K_{IR}) curve is underway, and similar methods will be employed to estimate mean and bounding curves for the dynamic data.

1. INTRODUCTION

The Heavy-Section Steel Technology (HSST) Program at Oak Ridge National Laboratory includes an ongoing assessment of the margins in reactor pressure vessel (RPV) integrity analyses. The establishment of pressure-temperature limits for RPV operation under the various postulated loading conditions is based on the K_{IR} curve in Section III of the ASME Boiler and Pressure Vessel Code.[1] The K_{IR} curve was constructed as a lower bound to dynamic initiation fracture toughness data, K_{Id}, and crack-arrest toughness data, K_{Ia}, from SA-533 grade B class 1, SA-508 class 2, and SA-508 class 3 steels and was published in Welding Research Council Bulletin 175[2] in 1972. The use of dynamic toughness data for establishment of the curve was apparently based on concerns about embrittled regions from which fracture may initiate and result in failure of

the vessel.[3] Therefore, the crack-arrest curve was adopted as a conservative measure. Section XI[4] of the Code is referenced in 10 CFR 50;[5] it was published in 1974, and Appendix A of that section included both K_{Ic} and K_{Ia} curves. The K_{Ia} curve is identical to the K_{IR} curve in Section III, while the K_{Ic} curve was constructed as a lower bound to the available static fracture toughness data for RPV steels. Basically, the K_{Ia} curve is used for normal loading conditions, while the K_{Ic} curve is used for emergency and faulted loading conditions. In 1978, the ASME Section XI Task Group on Flaw Evaluation published EPRI NP-719-SR, Flaw Evaluation Procedures: ASME Section XI (Ref. 6). That report includes the data used for construction of the K_{Ic} and K_{Ia} curves.

Use of the K_{IR} curve for establishment of the low-temperature overpressurization setpoint is beginning to constrain the operating window for some RPVs, and proposals have been made which essentially incorporate the use of the K_{Ic} curve for establishment of that setpoint. The margin-assessment task includes evaluation of local regions of low toughness ("local brittle zones"), evaluation of cleavage pop-ins during fracture toughness testing, and examination of the fracture toughness curves in Section XI of the Code. As a first step in the development of statistically-based fracture toughness curves, this letter report provides a preliminary review of the bases used for establishment of the existing K_{Ic} curve. Until recently, the K_{Ic} curves shown in the EPRI report and in Section XI of the Code were different, and those differences are discussed below. The data reported in EPRI NP-719-SR are reviewed and compared to the graphical plots in the EPRI report and in Appendix A of Section XI. Preliminary statistical analyses of the data are discussed and presented in the form of mean and confidence curves for comparison with the bounding curves in the Code.

2. COMPARISON OF THE EPRI AND ORIGINAL SECTION XI K_{Ic} CURVES

Use of the ASME curve is implied by 10 CFR 50 by virtue of its reference to Section XI of the ASME Code. *Regulatory Guide 1.154*,[7] however, refers the user to analytical programs, such as OCA-P,[8] which incorporate the EPRI curve. The Integrated Pressurized Thermal Shock Program,[9-11] for example, used OCA-P and, therefore, the EPRI equation as the basis for the K_{Ic} curves in those analyses. It was certainly very common practice to use the EPRI equation to represent the former ASME K_{Ic} curve, not only as an approximation, but because the belief was common that the EPRI curve and former ASME curve are the same. EPRI NP-719-SR shows the K_{Ic} data and provides the equation used to construct a curve (EPRI curve) as a lower boundary to the data base. The equation is as follows:

$$K_{Ic} = 33.2 + 2.806 \exp[0.02(T - RT_{NDT} + 100.0°F)] \ , \qquad (1)$$

where K_{Ic} is in ksi•√in., and T and RT_{NDT} are in °F. The same equation expressed in SI units is as follows:

$$K_{Ic} = 36.5 + 3.083 \exp[0.036(T - RT_{NDT} + 55.6°C)] \ , \qquad (2)$$

where K_{Ic} is in MPa•√m, and T and RT_{NDT} are in °C.

Prior to December 31, 1992, Appendix A of Section XI did not provide an equation to describe the K_{Ic} curve (ASME curve) shown in Fig. 1 (from Fig. A-4200-1 of Appendix A). It was apparently constructed manually. To compare the two curves, the

Code curve was digitized and plotted in Fig.1 with the K_{Ic} data and EPRI curve from EPRI NP-719-SR (the filled triangles labeled as A509 class 2 in the EPRI report should be A508 class 2). These data will be discussed later in this report. In Section XI, the ASME curve is plotted only over the temperature range shown in Fig. 1. The major differences between the ASME and EPRI curves occurs in the range from about 25 to 100 °F on the T-RT_{NDT} scale. The Code curve indicates higher K_{Ic} values in the range from about 65 to 200 ksi•√in. (71-220 MPa•√m). For example, at T - RT_{NDT} values of 50, 75, and 100 °F, the Code curve is about 12, 15, and 7 ksi•√in. (about 13, 12, and 4%) above the EPRI curve, respectively. In terms of temperature differences, at K_{Ic} values of 75, 100, and 150 ksi•√in. (82, 110, and 165 MPa•√m), the EPRI curve falls at higher temperatures by about 5, 8, and 6 °F (3, 4, and 3 °C), respectively.

Attempts were made to fit the digitized ASME Code curve data with an exponential equation of the same form as in Eq. (1) above, using a nonlinear regression routine, but the shape of the curve does not allow for a very good fit. The manual construction resulted in a "kink" in the curve. Sumio Yukawa,* however, developed an equation which he proposed for adoption by Section XI. The equation is as follows:

$$K_{Ic} = 33.2 + 23.0 \exp[0.021(T - RT_{NDT})] \ , \tag{3}$$

where K_{Ic} is in ksi•√in., and T and RT_{NDT} are in °F. The same equation expressed in SI units is as follows:

$$K_{Ic} = 36.5 + 25.3 \exp[0.038(T - RT_{NDT})] \ , \tag{4}$$

where K_{Ic} is in MPa•√m, and T and RT_{NDT} are in °C.

The Yukawa curve is also shown in Fig. 1. As can be seen, the Yukawa curve falls quite close to the ASME curve up to a K_{Ic} value of about 150 ksi•√in. and then rises more steeply. The curve was developed by simply setting the intercept value equal to that of the EPRI equation (33.2 ksi•√in.) and varying the other two constants until the curve fit the ASME curve reasonably well up to a T - RT_{NDT} value of about 75 °F.† Some examples of differences between the three curves are shown in Table 1.

Table 1. Comparison of fracture toughness curves

T - RT_{NDT} (°F)	K_{Ic} (ksi•√in.)		
	ASME	EPRI	Yukawa
50	101	89	99
75	141	126	144
100	193	186	221

* Committee correspondence from S. Yukawa, to R. C. Cipolla, Chairman, Working Group on Flaw Evaluation, Subject: Revision of Appendix A K_{Ic} curve and addition of equations, dated May 18, 1990.

† Personal communication between S. Yukawa and R. K. Nanstad (Oak Ridge National Laboratory), February 25, 1991.

Thus, relative to the ASME curve, the EPRI curve is more conservative and the Yukawa proposed curve is less conservative.

In the Heavy-Section Steel Irradiation (HSSI) Program, the primary objective of the Fifth Irradiation Series[12] is to investigate the effects of irradiation on the K_{Ic} curve in Section XI of the Code. Figures 2 and 3 show the unirradiated fracture toughness data for the two welds, 72W and 73W, in the Fifth Series, as well as the three curves shown in Fig. 1. Figure 4 shows the data for 72W and 73W on one plot. By using the EPRI curve, one result falls on the curve and none fall below. By using the former ASME curve, two results fall on the curve and two fall below. Those four are all from large specimens, 4-, 6- and 8-in.-thick compact specimens.

It is instructive to point out an important comparison of the data from the Fifth Series and the EPRI data. As shown in Fig. 1, the EPRI data do not extend beyond a $T - RT_{NDT}$ value of about 50 °F. Figure 1 gives the impression that the curves are overly conservative at $T - RT_{NDT}$ of about 50 °F and above. The data from the Fifth Series, however, extend to a $T - RT_{NDT}$ value of about 75 °F and show that none of the curves are overly conservative and, in fact, that the former ASME and Yukawa curves are nonconservative. A comparison of the data bases is shown in Fig. 5 to illustrate the point.

Regarding the irradiated results, Fig. 6 shows the data from both welds 72W and 73W. The RT_{NDT} of each weld has been adjusted upward in temperature equal to the irradiation-induced Charpy impact 30-ft-lb temperature shift. Relative to the three curves, eight results fall below the EPRI curve, 15 results fall below the former ASME curve, and 17 results fall below the Yukawa curve. Figure 7 shows the results on a reduced temperature scale for easier comparison.

The above information was included in the various ASME Code meetings, and in 1991 the Working Group on Flaw Evaluation of the Subgroup on Evaluation Standards in Section XI approved adoption of the EPRI equation as a replacement for the former ASME K_{Ic} curve. The changes were officially published in the 1992 Addenda to Section XI. The published equation is as follows:

$$K_{Ic} = 33.2 + 20.734 \exp[0.02(T - RT_{NDT})] \quad , \tag{5}$$

where K_{Ic} is in ksi•√in., and T and RT_{NDT} are in °F. Equation (5) is the same as Eq. (1) in a different factored form, and thus results in exactly the same curve.

3. EXAMINATION OF EPRI DATA BASE (EPRI NP-719-SR)

An initial examination was made of the EPRI data base (in Special Report EPRI NP-719-SR[6]) by comparing the data points for static fracture toughness in the plot of the K_{Ic} reference toughness curve, shown in Fig. 8 from Ref. 6, with the tabular data. The K_{Ic} reference toughness curve is evaluated from Eq. (1) [Eq. (5) can also be used]. There are several apparent inconsistencies, so the tabular data were checked with the original references[13-15] to the Westinghouse data. The EPRI tabular static fracture toughness data are basically correct, but contain five values that are typographical errors and two invalid values (by ASTM criteria for a valid K_{Ic} test). The comparison of the graphical plot of the supporting data for the K_{Ic} reference toughness curve in Ref. 6 and the data base indicates the following:

1. There is a +40 °F shift for some of the plotted data. The HSST-02 plate had different degrees of stress relieving with two resulting RT_{NDT}'s (0 °F and 40 °F). Initially, the HSST-02 plate data was plotted with an RT_{NDT} of 40 °F, but it was determined that

the RT_{NDT} of 0 °F was used to derive the K_{Ic} and K_{Ia} curves in the ASME Code. An errata was sent out on April 14,1980 with the correction for HSST-02 in the plot. The problem appears to be that in the new plot from the errata all the data points have been shifted +40 °F, not just the ones for HSST-02.

2. No data below $T\text{-}RT_{NDT} \approx -160$ °F are plotted. This leaves out the data for three sets of material completely [A533B Class 1 ($T\text{-}RT_{NDT}$ ranges from -215 to -385 °F), and HSST-01 and HSST-03 ($T\text{-}RT_{NDT} = -170$ °F)]. The HSST-01 and HSST-03 plates are listed in the legend, but no data for these plates are included in the plot. Several data points from other materials are also not plotted because of the low $T\text{-}RT_{NDT}$.

3. There are several data points in the plot which are not given in the data base, and there are data in the data base that are not in the plot.

A corrected data base has been generated from the same references[13-15] and is provided in Appendix A to this letter report. Figure 9 shows the data base with the K_{Ic} reference toughness curve. It is clear that the curve is not a lower bound to all the data.

4. LOWER-BOUND CURVE ESTIMATION TECHNIQUES

Three methods were used to develop lower-bound curves to the corrected K_{Ic} data base.

The first method of estimating a lower-bound curve was to simply adjust the EPRI K_{Ic} equation [see Eq. (1)] to include all the reported data. The resulting equation is given by

$$K_{Ic} = 23.7 + 4.0 \exp[0.02(T - RT_{NDT} + 100.0)] \ , \tag{6}$$

where K_{Ic} is in ksi•√in., and T and RT_{NDT} are in °F. A comparison of the curve generated from Eq. (6) and the corrected data base is shown in Fig. 10. It is interesting to note that the asymptotic value of 23.7 in Eq. (6) is less than the asymptotic value used in the K_{Ia} reference toughness curve, which is 26.8.

Rather than use an arbitrarily chosen curve, it is of interest to construct a statistically-based bounding curve. The second and third methods described herein used statistical approaches to generate bounding curves. The second method used a standard nonlinear regression technique to fit a mean curve with an exponential equation to the corrected data base. The form of the exponential equation is given by

$$K_{Ic} = A + B\exp[C(T - RT_{NDT})] \ , \tag{7}$$

where A = 36.68, B = 51.59, and C = 0.0115. This curve is shown in Fig. 11 with 95% and 99% confidence curves (confidence on the predicted value) and the EPRI curve from Eq. (1). The EPRI curve is close to the 99% confidence curve in the transition region, and within both confidence curves in the lower-shelf and upper-transition regions. The disadvantage of using this type of confidence curve is that there are no restrictions such as the recognition that K_{Ic} must be greater than zero or some positive value. Techniques are available for such analyses but have not yet been pursued. It is apparent from Fig. 11 that these confidence levels give unrealistic K_{Ic} values on the lower shelf.

The third method used to generate bounding curves to the corrected data base was a Weibull-based analysis using the Wallin procedure described in Refs. 16 and 17. Wallin has developed an analysis procedure that involves fitting a three-parameter Weibull

distribution to fracture toughness data at each temperature and also includes a size adjustment derived from a fixed Weibull slope concept. For this procedure, the K_{Ic} data was converted to SI units and adjusted to a 1T equivalence using the following equation

$$K_{Icx} = K_{min} + (K_{Ico} - K_{min})(B_o/B_x)^{0.25} \quad , \tag{8}$$

where K_{Icx} is the adjusted K_{Ic} for a specimen of thickness B_x, K_{Ico} is the observed K_{Ic} for a specimen of thickness B_o, and K_{min} is the lower limiting value of K_{Ic}. The three-parameter Weibull distribution function with fixed slope of 4 and K_{min} of 20 MPa•√m was then used to fit the data for each test temperature in the transition region, and T_o (temperature at which the mean fracture toughness is 100 MPa•√m) values were determined as in the Wallin[16] procedure to obtain a median curve ($K_{Ic\text{-median}}$) with the three-parameter exponential equation. This equation is given by

$$K_{Ic\text{-median}} = 30.0 + 70.0 \exp[0.019(T - T_o)] \quad , \tag{9}$$

where $K_{Ic\text{-median}}$ is in MPa•√m and T is in °C. The value of T_o, which is an average value of the T_o's in the transition range, for this evaluation of the adjusted data base was determined to be -16.5 °C (-29.7 °F). The adjusted data base (1T) with the curve generated from Eq. (9) are shown in Fig. 12. The same equation expressed in English units is as follows:

$$K_{Ic\text{-median}} = 27.27 + 63.6 \exp[0.01055(T - T_o)] \quad , \tag{10}$$

where $K_{Ic\text{-median}}$ is in ksi•√in. and T is in °F. Figure 13 shows the corrected data base with the mean curve, 95% and 99% confidence curves, and the EPRI K_{Ic} curve for comparison. The 99% confidence curve is close to the arbitrarily adjusted EPRI curve [Eq. (6)] on the lower shelf, and bounds all the data. Both confidence curves have lower slopes than the EPRI curve. A Weibull-based analysis provides reasonable lower-bound curves, but tends to be overly conservative at the higher toughness levels.

5. SUMMARY

The K_{Ic} curve in Article A-4000 of Appendix A, Section XI of the ASME Code is now the same as that given in the report, EPRI NP-719-SR. The manually constructed curve previously presented in Section XI was officially replaced on December 31, 1992, by publication of the 1992 Addenda to Section XI. The change also includes an analytical expression which, although factored differently than the expression contained in EPRI NP-719-SR, gives exactly the same K_{Ic} curve. For the K_{Ic} data plot in EPRI NP-719-SR, it appears that all the data points were shifted +40 °F in the April 14, 1980 errata, whereas only the data for HSST-02 Plate should have been shifted. In a comparison with the data contained in the original references, a few errors were found in the EPRI NP-719-SR tabular data. A corrected data base has been generated from those references. Furthermore, a large part of the data base is below $T - RT_{NDT} \approx -160$ °F, but these data are not included in the data plot which shows the K_{Ic} curve. A number of K_{Ic} results are substantially below the K_{Ic} curve.

A trial and error adjustment method was used to adjust the equation for the K_{Ic} curve so that all the data were bounded. The asymptotic value of that curve was 23.7 ksi•√in., which is significantly below 33.2 ksi•√in., the asymptotic value of the existing K_{Ic} curve. Two methods were used to develop statistically based bounding curves, a

standard nonlinear regression and a Weibull-based analysis which incorporates fixed values of the Weibull slope and K_{min}. The nonlinear regression provides confidence curves which are unrealistic in the lower temperature region. The Weibull-based procedure gives a 99% confidence curve which appears to be a good representation of a lower-bound curve to the data, but is overly conservative at the higher toughness values.

Further investigations in this area are underway and involve the collection of additional fracture toughness data, both valid K_{Ic} and elastic-plastic K_{Jc} results, to provide a larger data base and to evaluate the utility of K_{Jc} data in this regard (72W and 73W data). Additionally, a similar examination of the K_{Id} and K_{Ia} data used to construct the K_{Ia} (= K_{IR}) curve is underway and the same methods described above will be employed to estimate mean and bounding curves for the dynamic data.

6. REFERENCES

1. The American Society of Mechanical Engineers Boiler and Pressure Vessel Code, Section III, "Rules for Construction of Nuclear Power Plant Components, Division 1," 1992.

2. Welding Research Council, "PVRC Recommendations on Toughness Requirements for Ferritic Materials," Welding Research Council Bulletin 175, New York, August 1972.

3. Electric Power Research Institute, "White Paper on Reactor Vessel Integrity Requirements for Level A and B Conditions," EPRI TR-100251, Palo Alto, CA, January 1993.

4. The American Society of Mechanical Engineers Boiler and Pressure Vessel Code, Section XI, "Rules for Inservice Inspection of Nuclear Power Plant Components," 1992.

5. *Code of Federal Regulations*, Title 10, Part 50, January 1993.

6. The American Society of Mechanical Engineers Section XI Task Group on Flaw Evaluation, "Flaw Evaluation Procedures: ASME Section XI," EPRI NP-719-SR, Special Report, August 1978.

7. U. S. Nuclear Regulatory Commission, *Regulatory Guide 1.154*, "Format and Content of Plant-Specific Pressurized Thermal Shock Safety Analysis Reports for Pressurized Water Reactors," January 1987.

8. R. D. Cheverton and D. G. Ball, Martin Marietta Energy Systems, Inc., Oak Ridge Natl. Lab., "OCA-P, A Deterministic and Probabilistic Fracture-Mechanics Code for Application to Pressure Vessels," NUREG/CR-3618 (ORNL-5991), May 1984.

9. D. L. Selby et al., Martin Marietta Energy Systems, Inc., Oak Ridge Natl. Lab., "Pressurized-Thermal-Shock Evaluation of the H. B. Robinson Nuclear Power Plant," NUREG/CR-4183, Vol. 1 (ORNL/TM-9567/V1), September 1985.

10. D. L. Selby et al., Martin Marietta Energy Systems, Inc., Oak Ridge Natl. Lab., "Pressurized-Thermal-Shock Evaluation of the Calvert Cliffs Unit 1 Nuclear Power Plant," NUREG/CR-4022 (ORNL/TM-9408), September 1985.

11. T. J. Burns et al., Martin Marietta Energy Systems, Inc., Oak Ridge Natl. Lab., "Preliminary Development of an Integrated Approach to the Evaluation of Pressurized-Thermal-Shock as Applied to the Oconee Unit 1 Nuclear Power Plant," NUREG/CR-3770 (ORNL/TM-9176), May 1986.

12. R. K. Nanstad et al., Martin Marietta Energy Systems, Inc., Oak Ridge Natl. Lab., "Irradiation Effects on Fracture Toughness of Two High-Copper Submerged-Arc Welds, HSSI Series 5," USNRC Report NUREG/CR-5913 (ORNL/TM-12156/V1), October 1992.

13. W. O. Shabbits, W. H. Pryle, and E. T. Wessel, *Heavy Section Fracture Toughness Properties of A533, Grade B, Class-1 Steel Plate and Submerged Arc Weldment*, HSST Technical Report 6, WCAP-7414, December 1969.

14. T. R. Mager, *Fracture Toughness Characterization Study of A533, Grade B, Class-1 Steel*, HSST Technical Report 10, WCAP-7578, October 1970.

15. T. R. Mager, F. O. Thomas, and W. S. Hazelton, *Evaluation by Linear Elastic Fracture Mechanics of Radiation Damage to Pressure Vessel Steels*, HSST Technical Report 5, WCAP-7328, Revised, October 1969.

16. K. Wallin, "The Scatter in K_{Ic}-Results," *Eng. Frac. Mech.*, **19(6)**, 1085-1093, 1984.

17. K. Wallin, "The Size Effect in K_{Ic}-Results," *Eng. Frac. Mech.*, **22(1)**, 149-63, 1985.

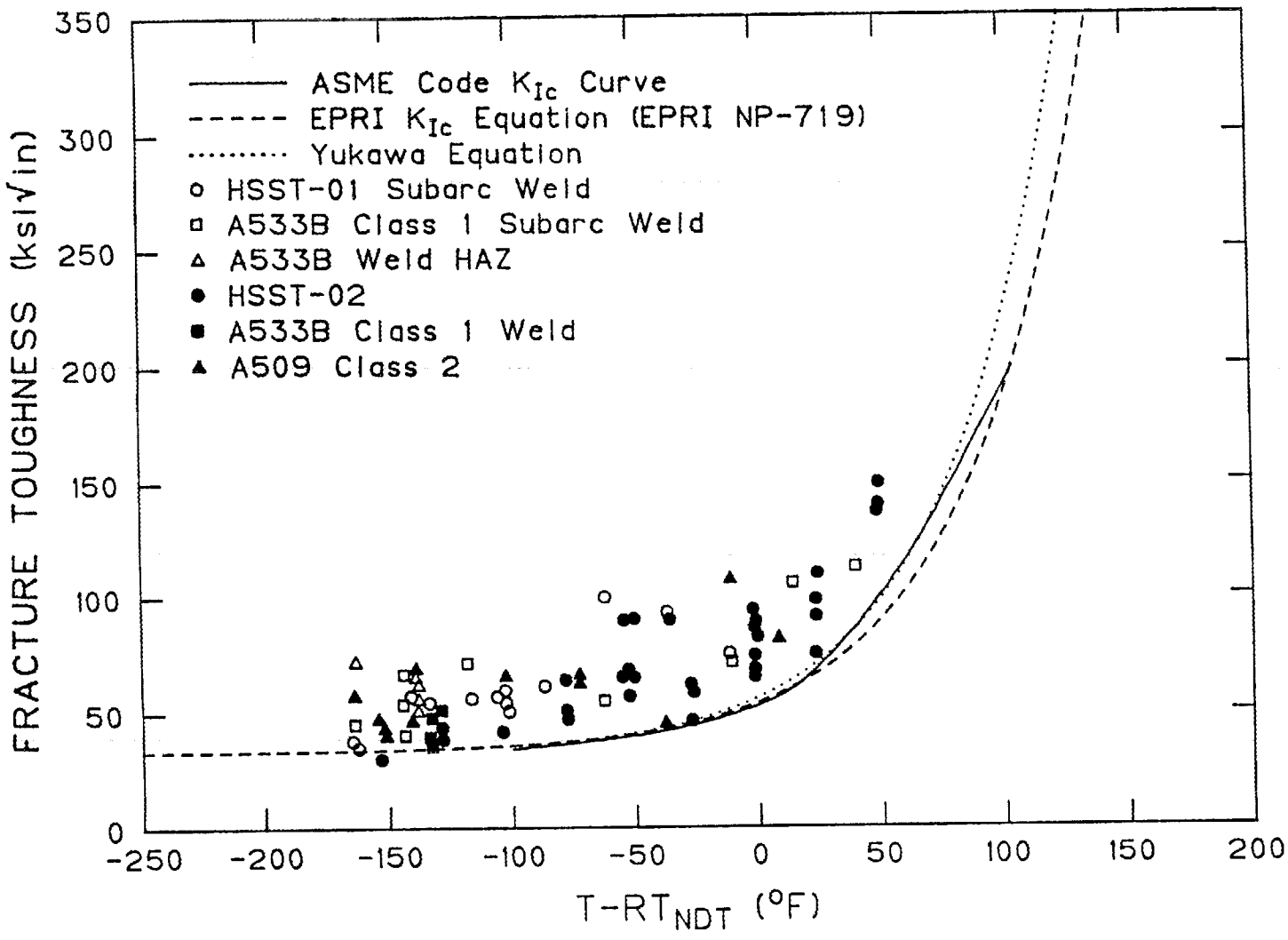

Fig. 1. Comparison of the EPRI, ASME Code Section XI, and Yukawa proposed curves relative to the K_{Ic} data from EPRI NP-719-SR.

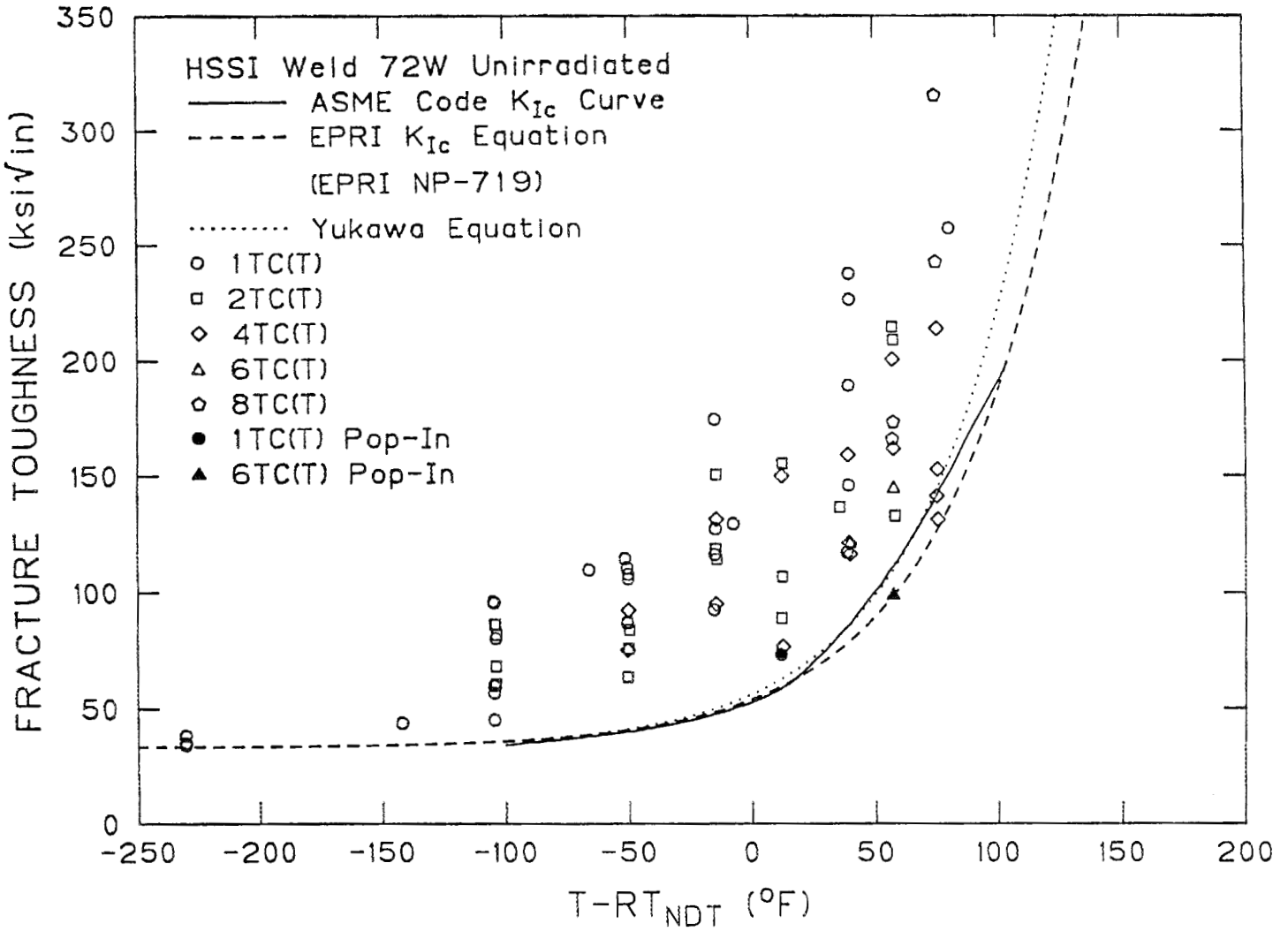

Fig. 2. Comparison of the EPRI, ASME Code Section XI, and Yukawa proposed curves relative to the K_{Jc} data from unirradiated HSSI Weld 72W.

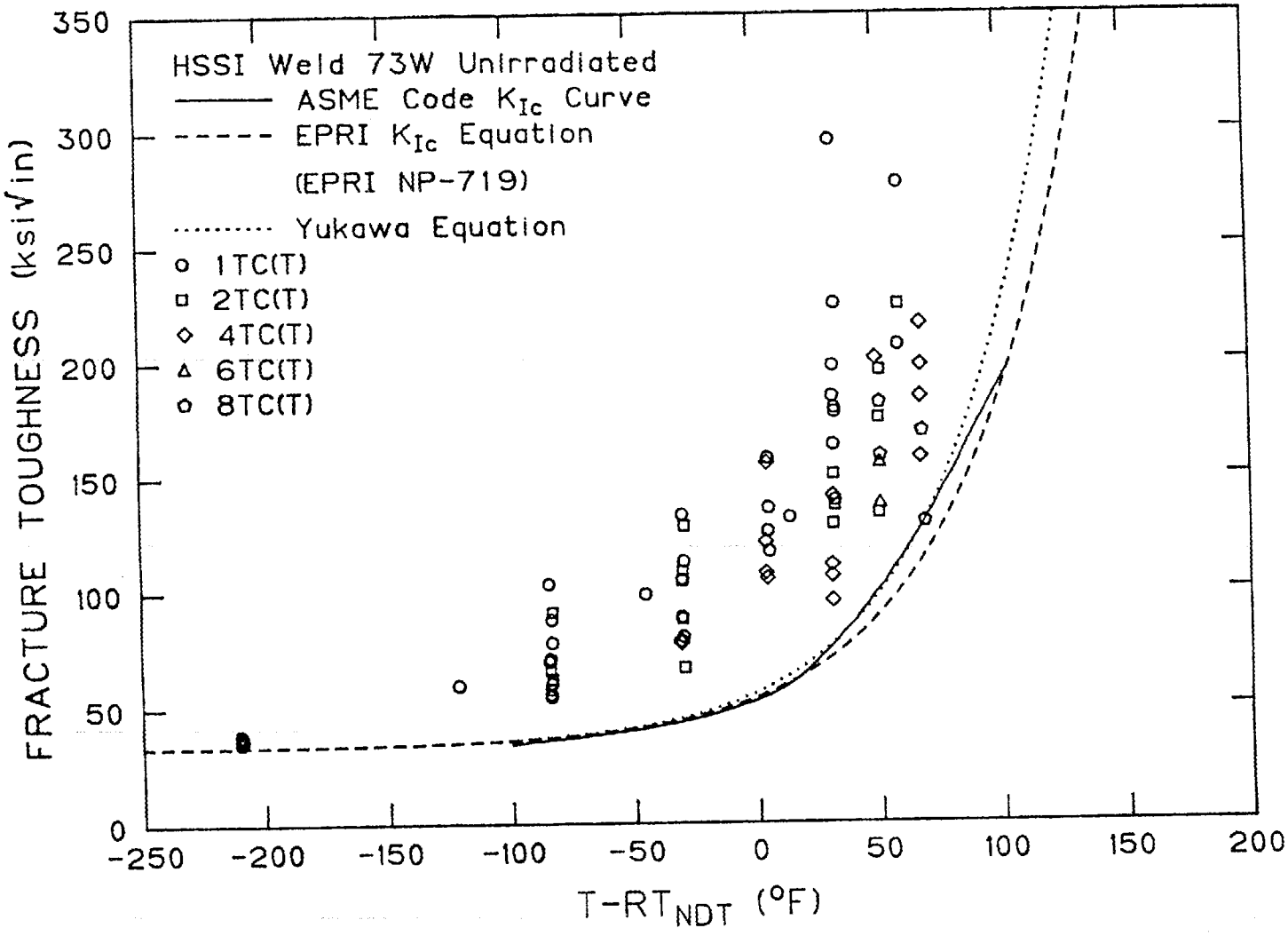

Fig. 3. Comparison of the EPRI, ASME Code Section XI, and Yukawa proposed curves relative to the K_{Jc} data from unirradiated HSSI Weld 73W.

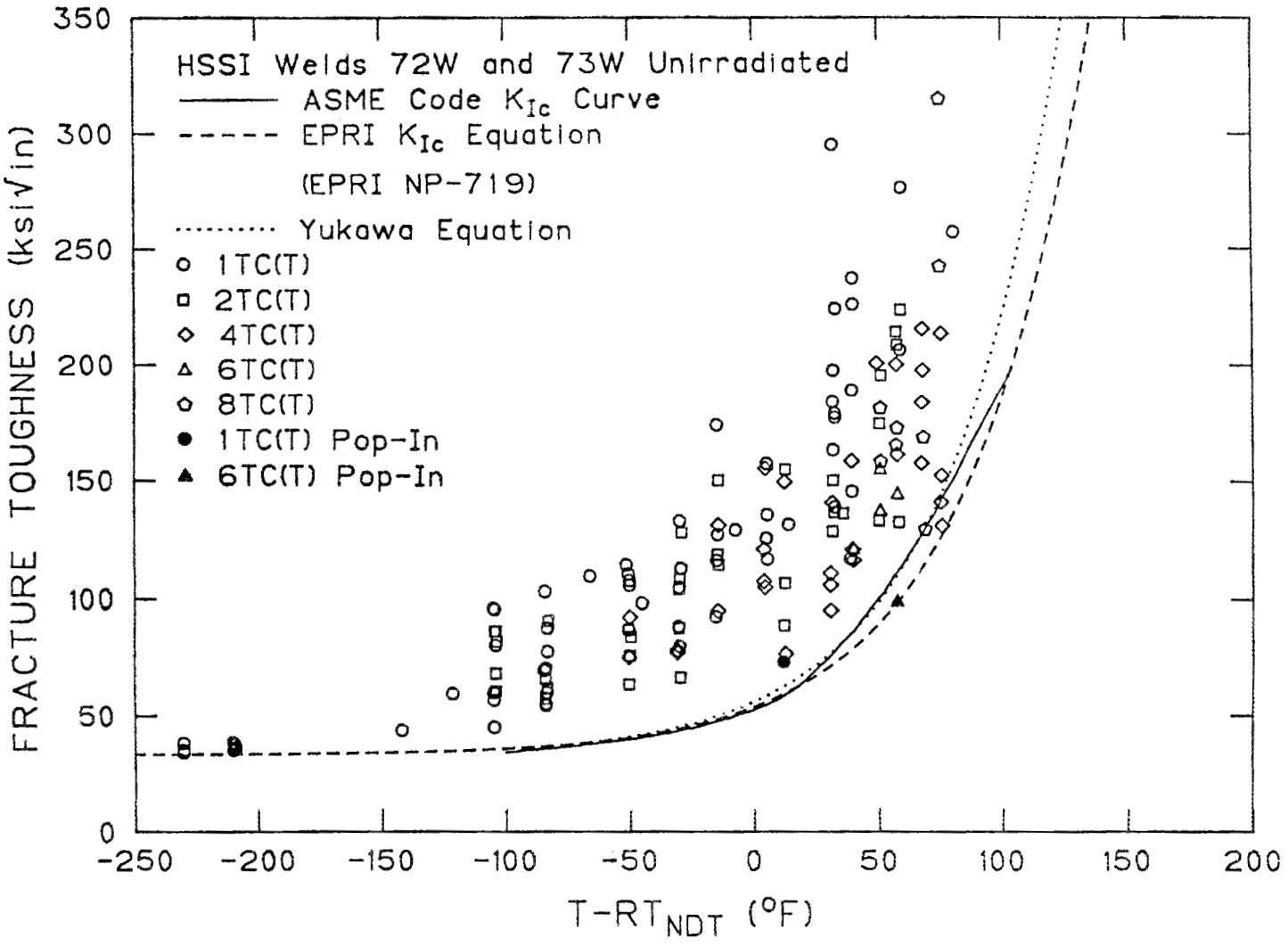

Fig. 4. Comparison of the EPRI, ASME Code Section XI, and Yukawa proposed curves relative to the K_{Jc} data from unirradiated HSSI Welds 72W and 73W.

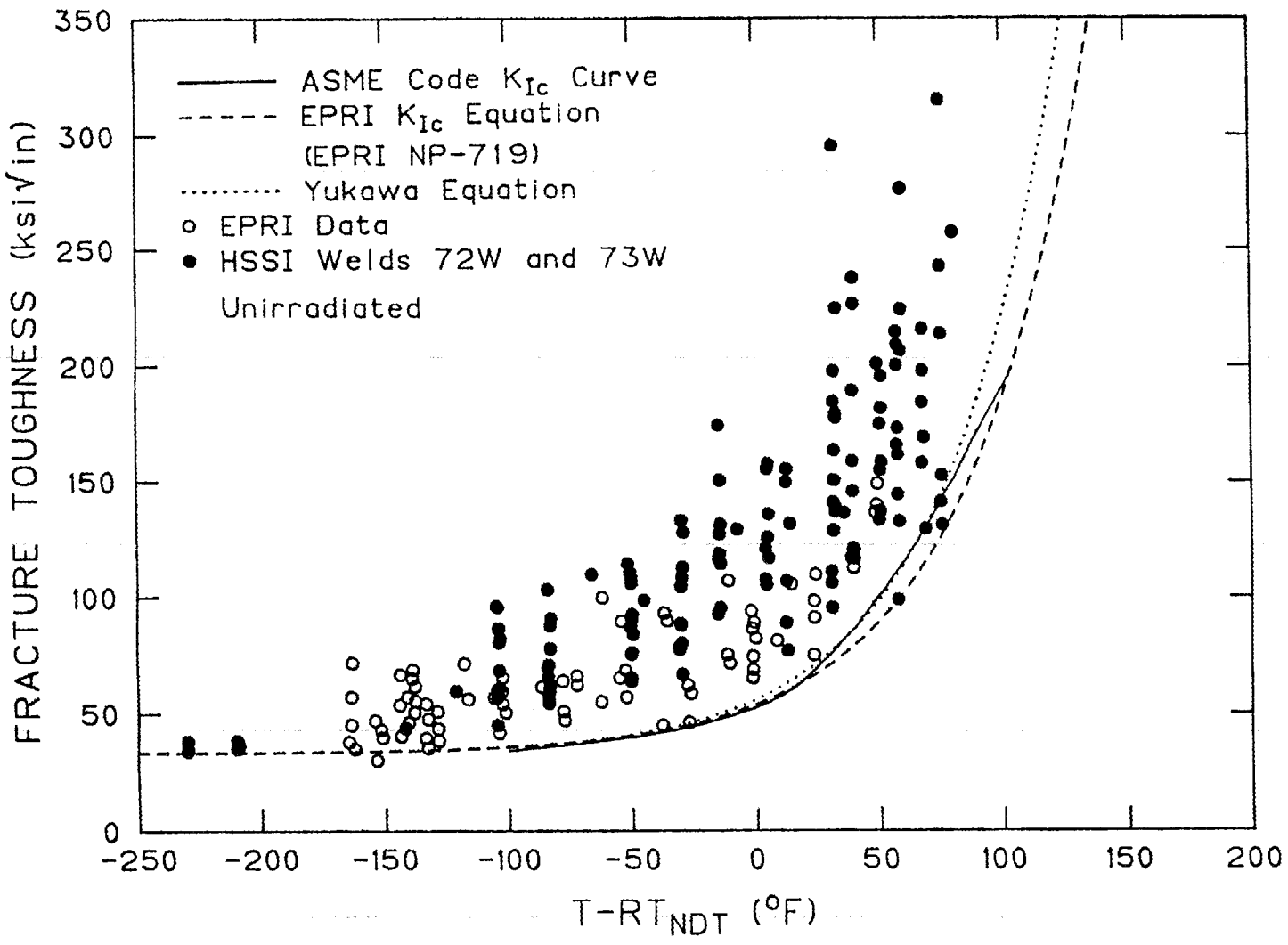

Fig. 5. Comparison of the EPRI, ASME Code Section XI, and Yukawa proposed curves relative to the K_{Jc} data from unirradiated HSSI Welds 72W and 73W and the K_{Ic} data from EPRI NP-719-SR.

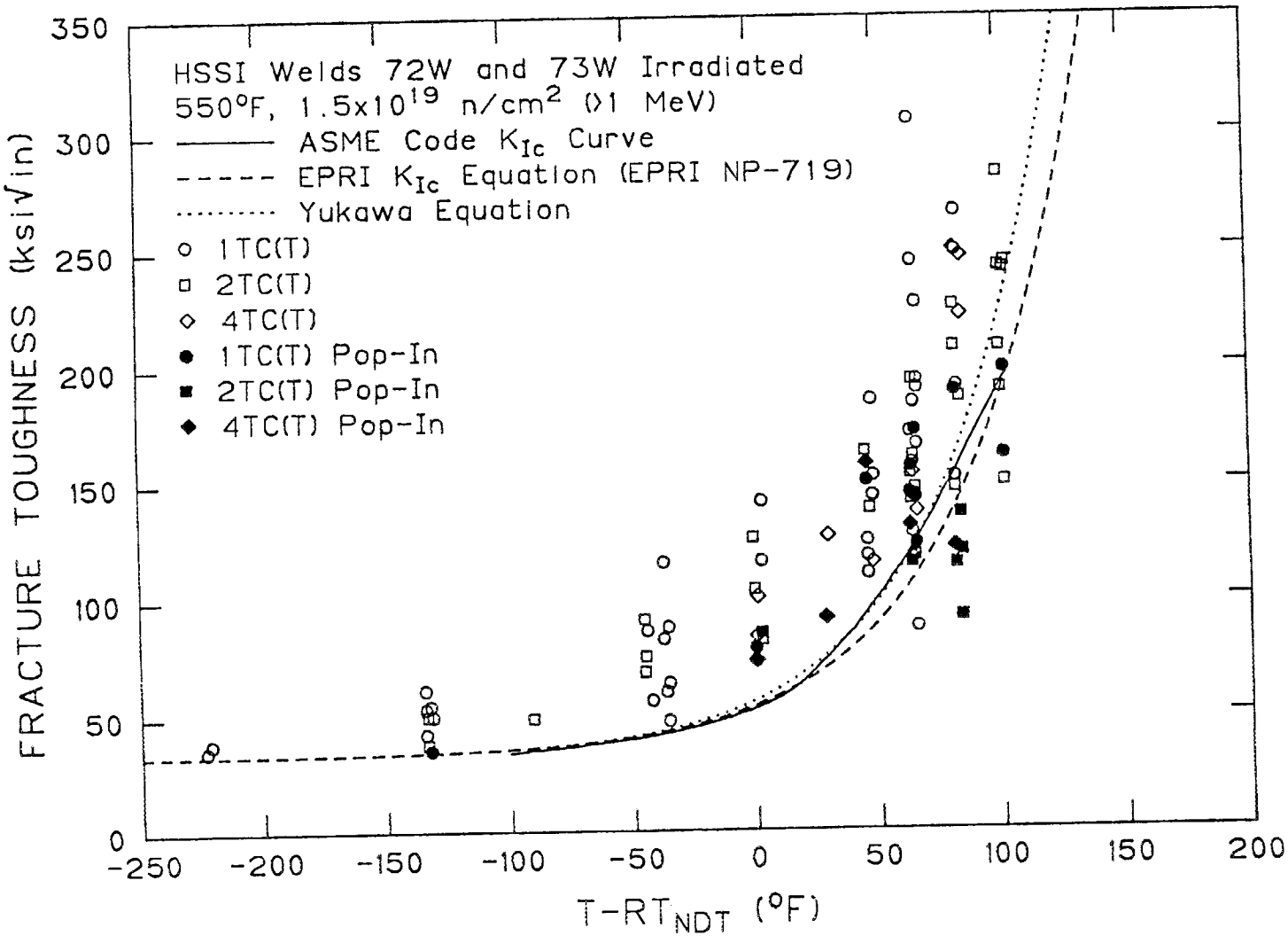

Fig. 6. Comparison of the EPRI, ASME Code Section XI, and Yukawa proposed curves relative to the K_{Jc} data from irradiated HSSI Welds 72W and 73W. The T - RT_{NDT} scale is from -250 to 200 °F.

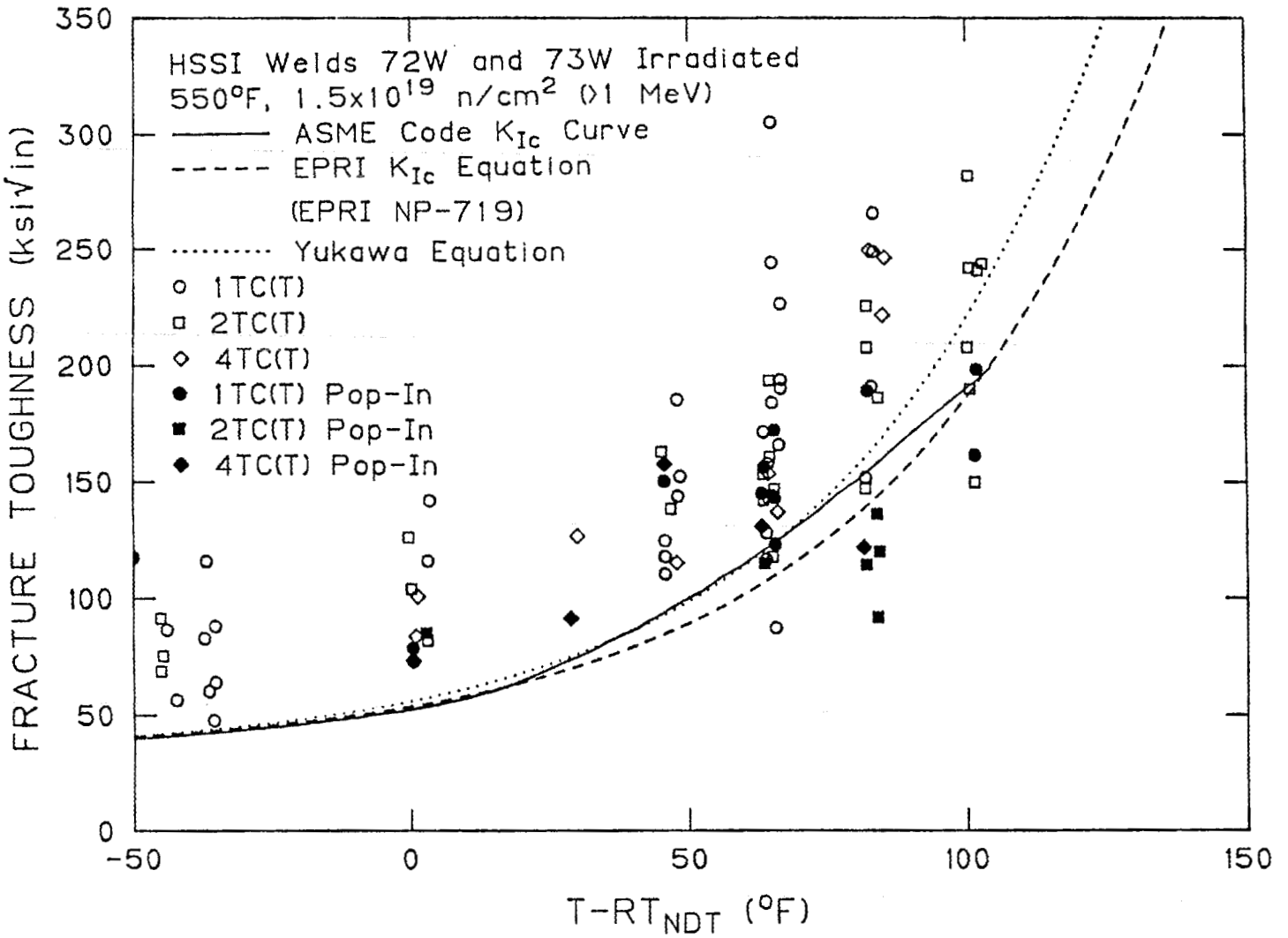

Fig. 7. Comparison of the EPRI, ASME Code Section XI, and Yukawa proposed curves relative to the K_{Jc} data from irradiated HSSI Welds 72W and 73W. The T - RT_{NDT} scale is from -50 to 150 °F.

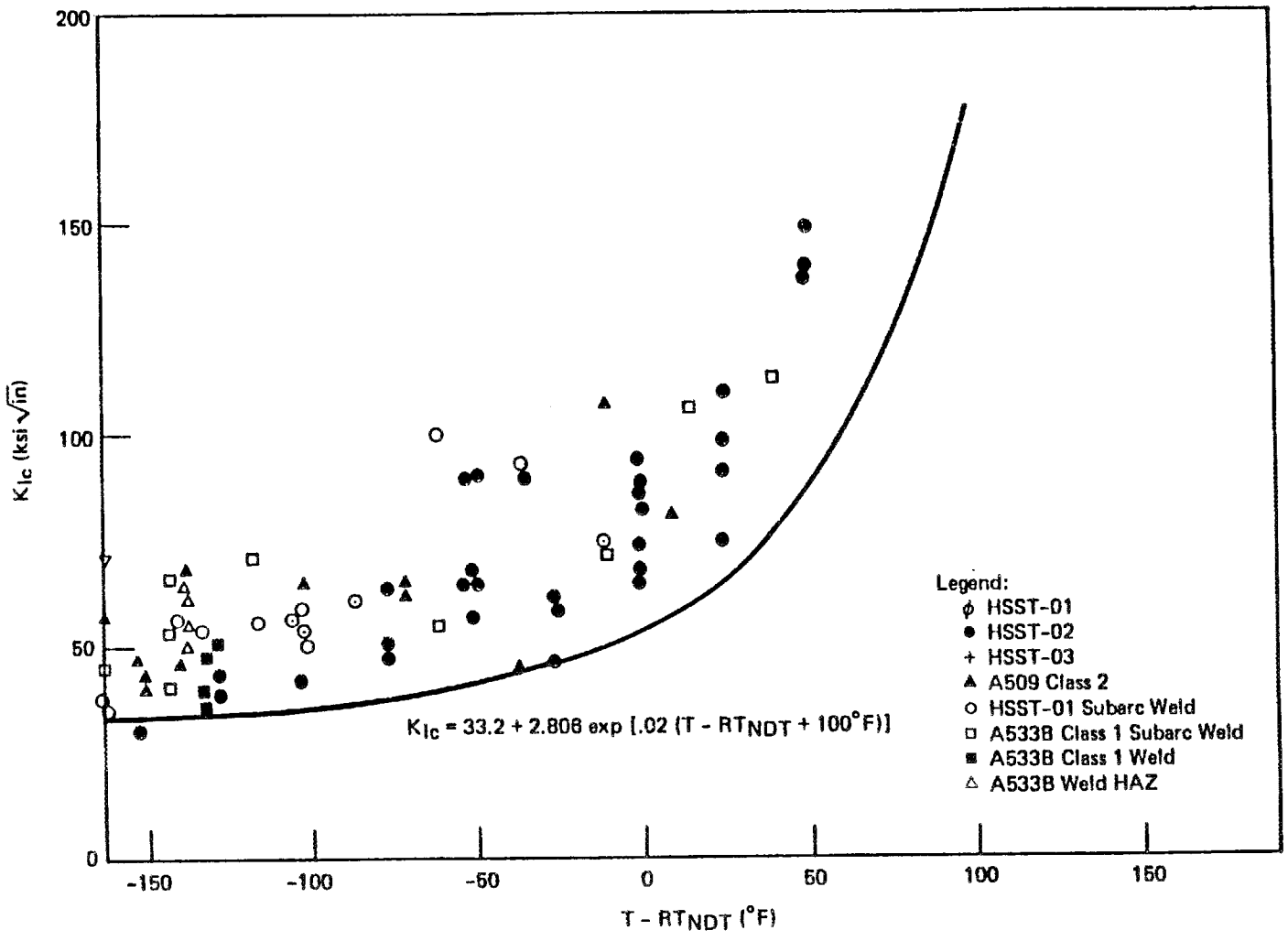

Fig. 8. K_{Ic} reference toughness curve with supporting data from EPRI NP-719-SR.

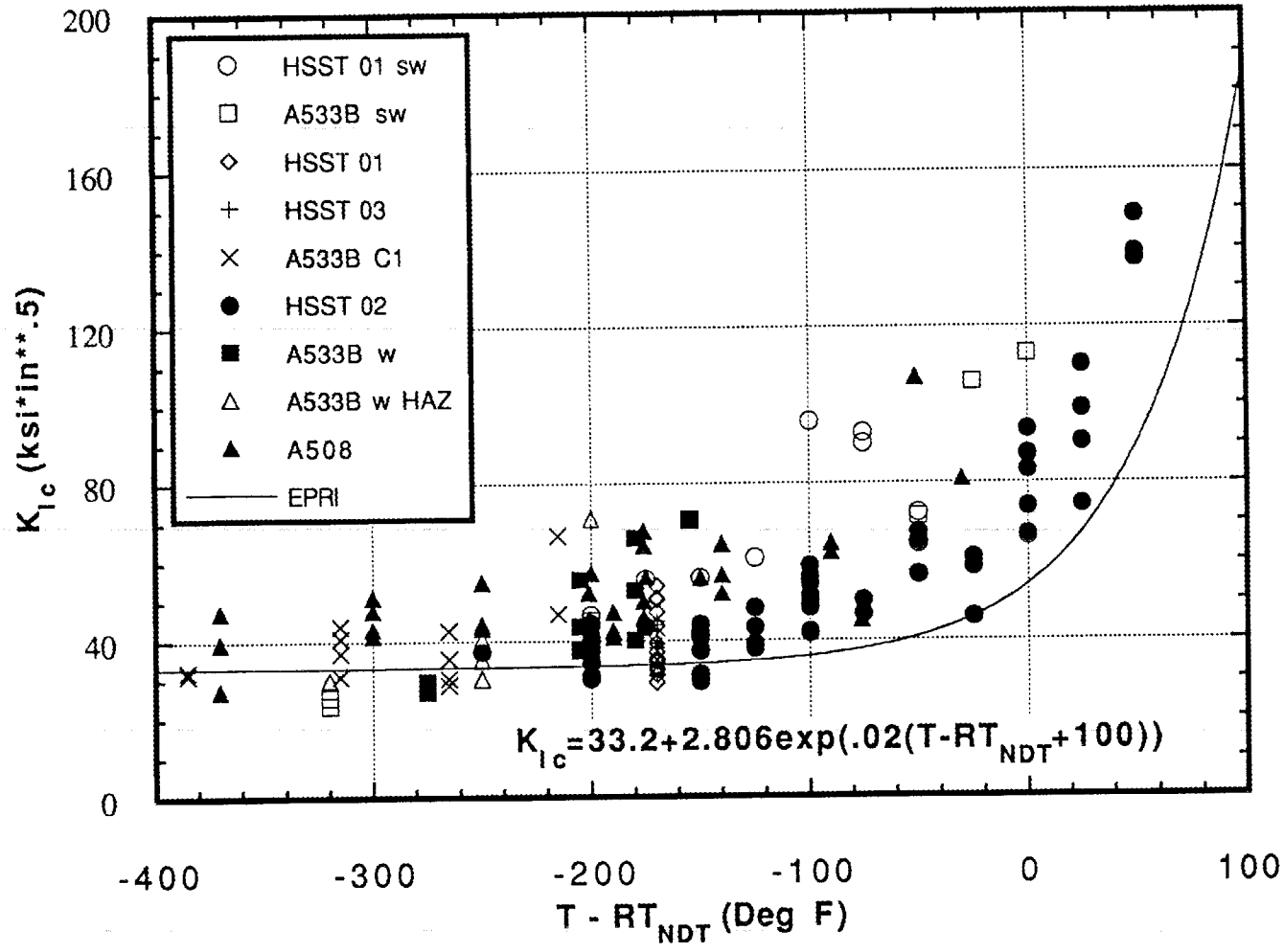

Fig. 9. K_{Ic} reference toughness curve with EPRI data base indicates that the curve is not a lower bound to all the data.

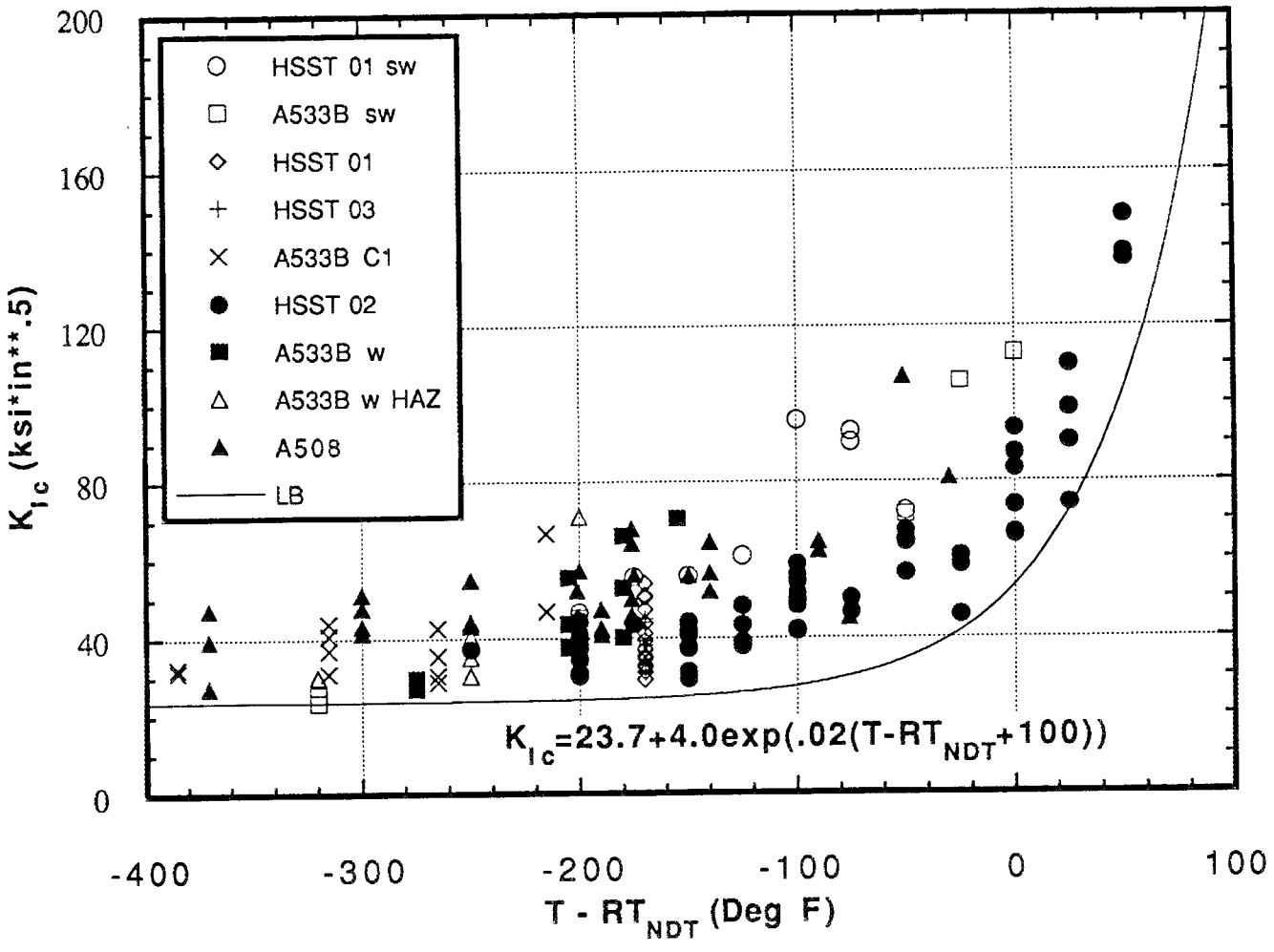

Fig. 10. Arbitrarily adjusted K_{Ic} curve with EPRI data base has an asymptotic value less than the K_{Ia} reference toughness curve.

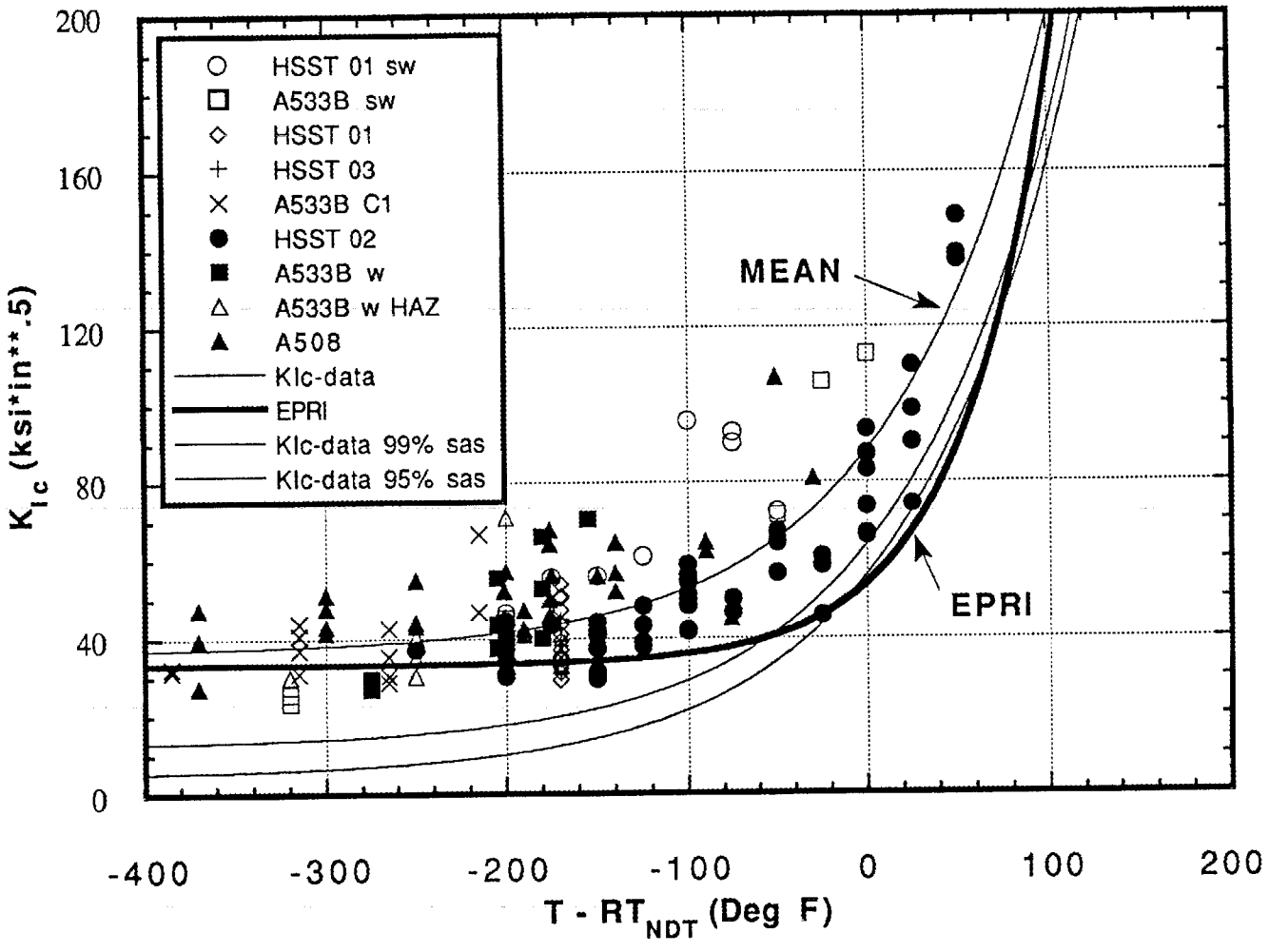

Fig. 11. A mean curve fit to the EPRI data base with 95% and 99% confidence curves gives unrealistic bounding curves in the lower-shelf region.

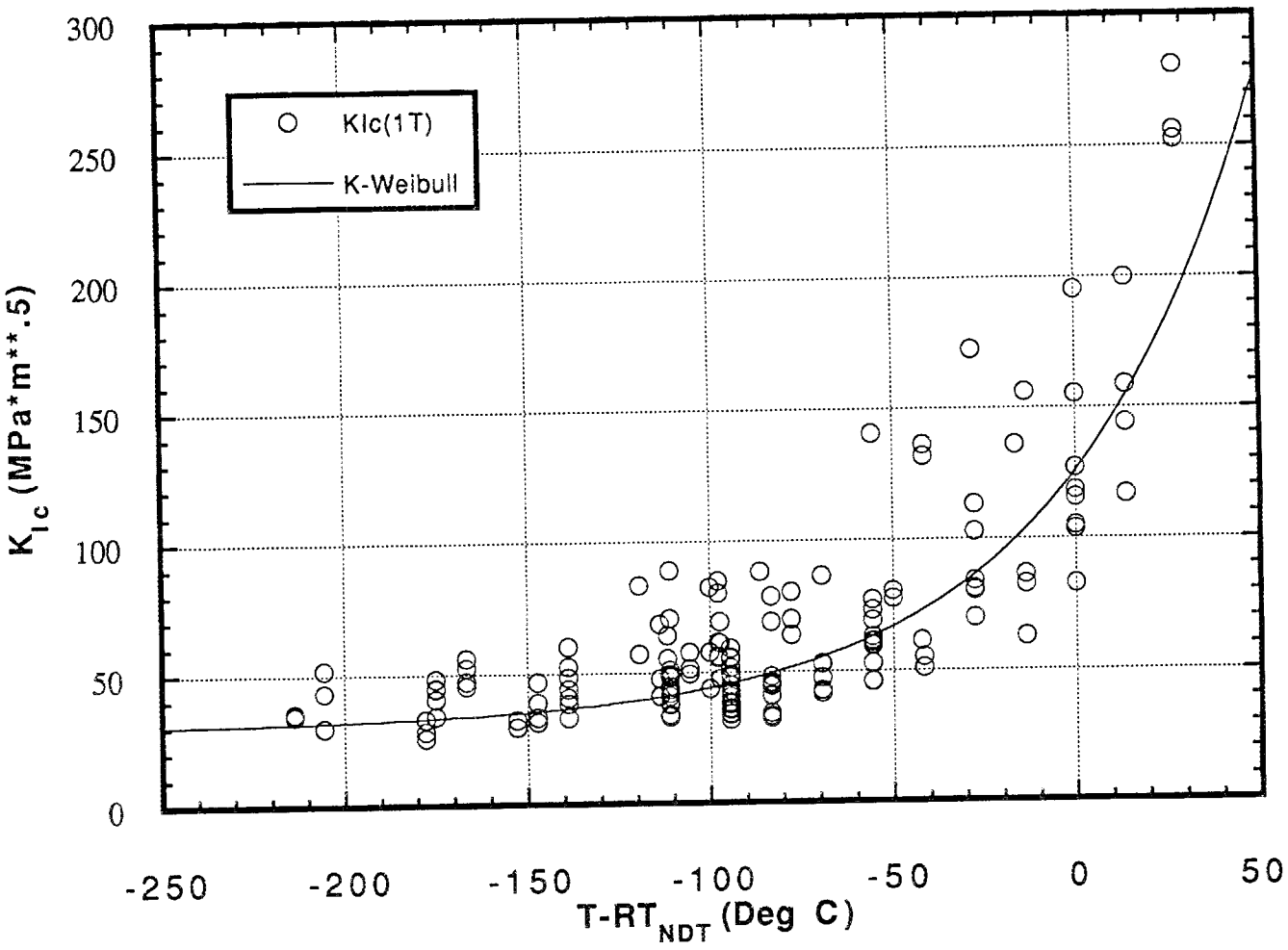

Fig. 12. A Weibull analysis of the adjusted (1T equivalence) EPRI data base using the Wallin method.

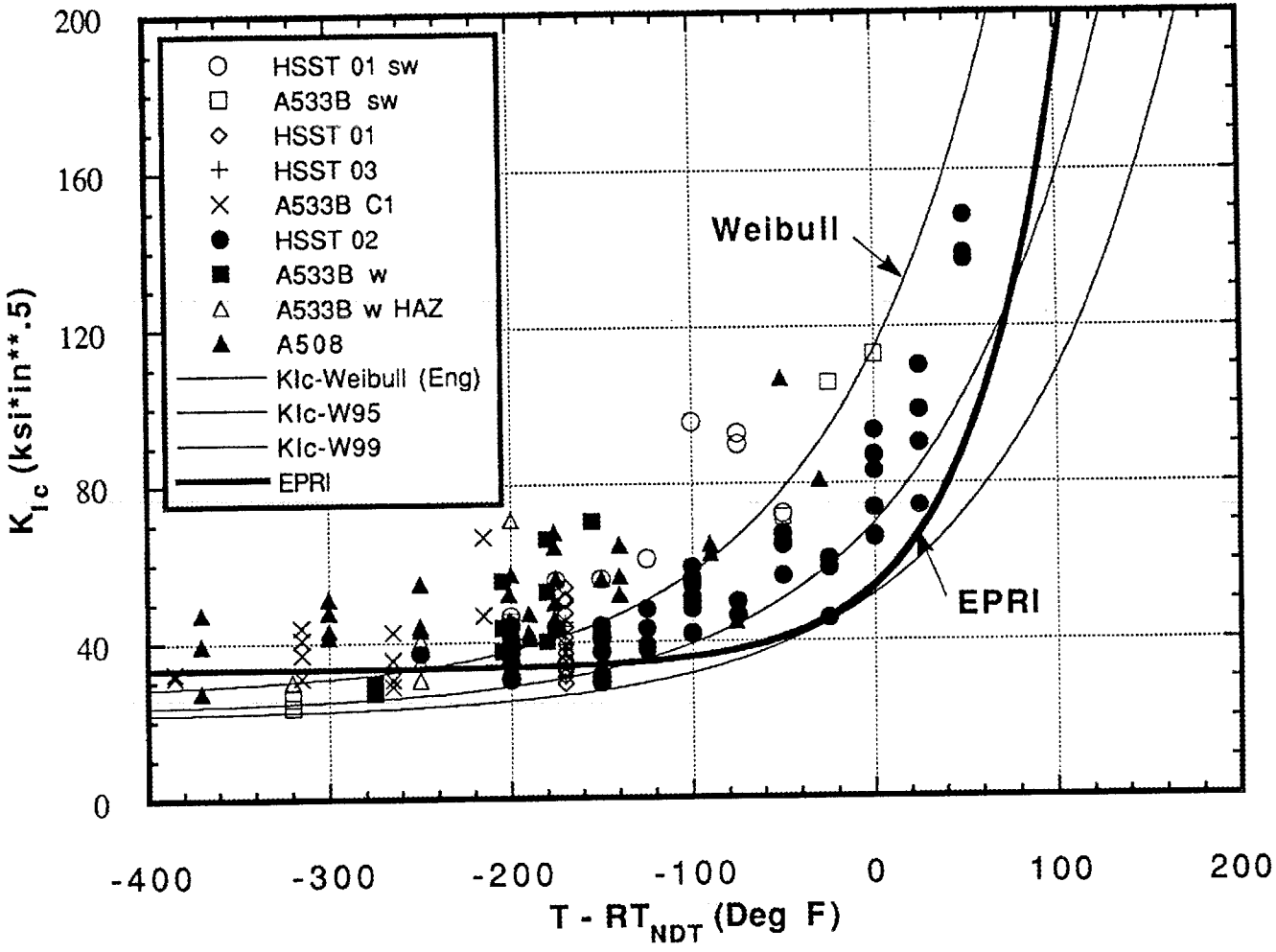

Fig. 13. A Weibull analysis of the EPRI data base using the Wallin method gives a 99% confidence curve which bounds all the data.

Appendix A

EPRI Data Base

EPRI Data Base

Material	Specimen Size	Orientation	Temp (Deg F)	RTNDT (Deg F)	T - RTNDT (Deg F)	Klc (ksi√in)
HSST 01	1T-CT		-200	0	-200	46.6
subarc weld	1T-CT		-175	0	-175	55.8
	4T-CT		-150	0	-150	56.1
	4T-CT		-125	0	-125	61.1
	4T-CT		-100	0	-100	96
	4T-CT		-75	0	-75	90.3
	4T-CT		-75	0	-75	93.1
	6T-CT		-50	0	-50	72.6
A533B Class 1	1T-CT		-200	0	-200	35.1
subarc weld	1T-CT		-200	0	-200	45.2
	1T-CT		-320	0	-320	25.9
	1T-CT		-320	0	-320	23.7
	4T-CT		-100	0	-100	55.2
	4T-CT		-50	0	-50	71.6
	4T-CT		-25	0	-25	105.9
	8T-CT		0	0	0	113.1
HSST 01	1T-CT	RW	-150	20	-170	43.9
	1T-CT	RW	-150	20	-170	39.4
	1T-CT	RW	-150	20	-170	31.3
	1T-CT	RW	-150	20	-170	47.3
	1T-CT	RW	-150	20	-170	50.4
	1T-CT	RW	-150	20	-170	41.2
	1T-CT	RW	-150	20	-170	54
	1T-CT	RW	-150	20	-170	50.9
	1T-CT	RW	-150	20	-170	35.5
	1T-CT	RW	-150	20	-170	33.2
	1T-CT	RW	-150	20	-170	37.2
	1T-CT	RW	-150	20	-170	37.1
	1T-CT	RW	-150	20	-170	37.1
	1T-CT	RW	-150	20	-170	34.7
	1T-CT	RW	-150	20	-170	35
	1T-CT	RW	-150	20	-170	32.6
	1T-CT	RW	-150	20	-170	29.4
HSST 03	1T-CT	RW	-150	20	-170	44
	1T-CT	RW	-150	20	-170	31.4
	1T-CT	RW	-150	20	-170	39.3
	1T-CT	RW	-150	20	-170	31.3
	1T-CT	RW	-150	20	-170	33
	1T-CT	RW	-150	20	-170	38.1
	1T-CT	RW	-150	20	-170	31.1
	1T-CT	RW	-150	20	-170	44.9
	1T-CT	RW	-150	20	-170	39.4
A533B Class 1	1X-WOL	RW	-320	65	-385	31.6

	1T-WOL	RW	-320	65	-385	32.5
	1X-WOL	RW	-250	65	-315	40.9
	1X-WOL	RW	-250	65	-315	37.1
	1X-WOL	RW	-250	65	-315	44
	1T-WOL	RW	-250	65	-315	40.8
	1T-WOL	RW	-250	65	-315	31.2
	1X-WOL	RW	-200	65	-265	30.6
	1X-WOL	RW	-200	65	-265	29
	1T-WOL	RW	-200	65	-265	35.6
	1T-WOL	RW	-200	65	-265	42.8
	2T-WOL	RW	-150	65	-215	46.9
	2T-WOL	RW	-150	65	-215	66.9
HSST 02	1X-WOL	RW	-200	0	-200	30.5
(Mager)	1X-WOL	RW	-200	0	-200	37.5
	1X-WOL	RW	-200	0	-200	41
	1T-WOL	RW	-200	0	-200	31.2
	1T-WOL	RW	-200	0	-200	30.8
	1T-WOL	RW	-175	0	-175	43.5
	1X-WOL	RW	-150	0	-150	29.7
	1X-WOL	RW	-150	0	-150	31.5
	1X-WOL	RW	-150	0	-150	41.2
	1X-WOL	RW	-150	0	-150	30.5
	1X-WOL	RW	-125	0	-125	39.1
	1T-WOL	RW	-125	0	-125	48.3
	1T-WOL	RW	-125	0	-125	43.4
	1T-WOL	RW	-125	0	-125	38.1
	2T-WOL	RW	-100	0	-100	51.4
	2T-WOL	RW	-100	0	-100	59
	2T-WOL	RW	-100	0	-100	56.2
	2T-WOL	RW	-100	0	-100	50.2
	2T-WOL	RW	-50	0	-50	65.1
	2T-WOL	RW	-50	0	-50	65
	2T-WOL	RW	-50	0	-50	67.5
	2T-WOL	RW	-50	0	-50	65
	1X-WOL	RW	-250	0	-250	37.3
	1X-WOL	RW	-200	0	-200	44
	1X-WOL	RW	-200	0	-200	34.6
	1X-WOL	RW	-200	0	-200	39.9
	1X-WOL	RW	-200	0	-200	38.5
	1T-CT	RW	-150	0	-150	42.1
	1T-CT	RW	-150	0	-150	37.7
	1T-CT	RW	-150	0	-150	40.7
	1T-CT	RW	-100	0	-100	42.2
	1T-CT	RW	-100	0	-100	48.5
	1T-CT	RW	-100	0	-100	48.5
	1T-CT	RW	-75	0	-75	50.3

EPRI Data Base

	1T-CT	RW	-75	0	-75	46.6
	1T-CT	RW	-100	0	-100	54.8
	1T-CT	RW	-100	0	-100	54.4
	2T-WOL	RW	-50	0	-50	56.7
	2T-WOL	RW	0	0	0	66.4
	2T-WOL	RW	0	0	0	93.7
	2T-WOL	RW	0	0	0	83.4
A533B Class 1	1X-WOL		-320	-45	-275	29.7
weld	1X-WOL		-320	-45	-275	27.2
	1X-WOL		-250	-45	-205	37.6
	1X-WOL		-250	-45	-205	37.8
	1T-WOL		-250	-45	-205	43.6
	2T-WOL		-250	-45	-205	55.6
	1T-WOL		-225	-45	-180	40.1
	1T-WOL		-225	-45	-180	52.8
	2T-WOL		-225	-45	-180	66.2
	2T-WOL		-200	-45	-155	70.7
A533B Class 1	1X-WOL		-320	0	-320	30.3
weld-HAZ	1X-WOL		-250	0	-250	35.2
	1X-WOL		-250	0	-250	40.4
	1T-WOL		-250	0	-250	30.5
	1T-WOL		-250	0	-250	44.2
	2T-WOL		-200	0	-200	71.2
A508 Class 2	1X-WOL		-320	50	-370	39.6
European	1X-WOL		-320	50	-370	27.5
Forging	1T-WOL		-320	50	-370	47.5
	1X-WOL		-250	50	-300	43.2
	1X-WOL		-250	50	-300	47.9
	1X-WOL		-250	50	-300	41.6
	1T-WOL		-250	50	-300	51.3
	1T-WOL		-200	50	-250	55
	2T-WOL		-200	50	-250	43.3
	2T-WOL		-150	50	-200	57.2
	2T-WOL		-125	50	-175	56.2
	2T-WOL		-100	50	-150	56
HSST 02	6T-CT	RW	25	0	25	98.9
(Shabbits)	6T-CT	RW	25	0	25	74.5
	6T-CT	RW	25	0	25	90.5
	6T-CT	RW	0	0	0	73.9
	6T-CT	RW	0	0	0	66.9
	11T-CT	RW	50	0	50	148.6
	10T-CT	RW	50	0	50	137.3
	10T-CT	RW	50	0	50	139
	4T-CT	RW	0	0	0	87.2
	4T-CT	RW	-25	0	-25	61
	4T-CT	RW	-25	0	-25	58.7

	4T-CT	RW	-25	0	-25	45.9
	10T-CT	RW	0	0	0	87.5
	10T-CT	RW	25	0	25	110.3
	1T-CT	RW	-250	0	-250	37.3
	1T-CT	RW	-200	0	-200	44.4
	1T-CT	RW	-200	0	-200	34.6
	1T-CT	RW	-200	0	-200	39.9
	1T-CT	RW	-200	0	-200	34.8
	1T-CT	RW	-150	0	-150	44.1
	1T-CT	RW	-150	0	-150	37.4
	1T-CT	RW	-150	0	-150	41.8
	1T-CT	RW	-100	0	-100	48.3
	1T-CT	RW	-100	0	-100	48.3
	1T-CT	RW	-100	0	-100	41.9
	2T-CT	RW	-100	0	-100	49.7
	2T-CT	RW	-50	0	-50	64.6
	2T-CT	RW	-50	0	-50	64.7
A508 Class 2	2T-CT		-150	51	-201	52.2
(unpublished)	2T-CT		-150	51	-201	45.5
	2T-CT		-125	51	-176	46
	2T-CT		-125	51	-176	64.3
	2T-CT		-125	51	-176	50
	4T-CT		-25	51	-76	45
	6T-CT		0	51	-51	107
	2T-CT		-125	51	-176	45.6
	2T-CT		-125	51	-176	68
A508 Class 2	2T-CT		-75	65	-140	52
(unpublished)	2T-CT		-75	65	-140	64.6
	2T-CT		-75	65	-140	56.6
	2T-CT		-25	65	-90	64.7
	2T-CT		-25	65	-90	62.4
	8T-CT		35	65	-30	81
	2T-CT		-125	65	-190	47.2
	2T-CT		-125	65	-190	40.9
	2T-CT		-125	65	-190	42.5
	2T-CT		-125	65	-190	42.5

DISTRIBUTION

1. D. J. Alexander
2. B. R. Bass
3. J. W. Bryson
4. R. D. Cheverton
5. W. R. Corwin
6. D. F. Craig
7. J. S. Crowell
8. T. L. Dickson
9. E. M. Hackett, NRC
10. F. M. Haggag
11. H. W. Hayden, Jr.
12. A. L. Hiser
13. S. K. Iskander

14-18. J. A. Keeney

19. W. J. McAfee

20-24. D. E. McCabe

25-26. S. N. M. Malik, NRC

27. M. E. Mayfield, NRC
28. J. G. Merkle

29-33. R. K. Nanstad

34. D. G. O'Connor

35-36. W. E. Pennell

37. C. E. Pugh
38. C. Z. Serpan, Jr., NRC
39. D. K. M. Shum
40. R. E. Stoller
41. R. L. Swain
42. T. J. Theiss
43. G. E. Whitesides
44. Laboratory–RC